

Strength of the double-phonon state within an exactly solvable model

Nguyen Dinh Dang*

*RI-beam Factory Project Office, RIKEN, 2-1 Hirosawa, Wako, 351-0198 Saitama, Japan
and Institute for Nuclear Science and Technique, VAEC, Hanoi, Vietnam*

(Received 16 October 2001; published 4 March 2002)

The deviation of the energy-weight sum rule (EWSR) and the energy shift for the two-phonon state from the prediction of the independent-phonon picture (the harmonic limit) are studied within the exactly solvable Lipkin-Meskov-Glick model. The exact results are used to compare with the estimations given within the random-phase approximation (RPA) and the renormalized RPA (RRPA). The analysis of the numerical results shows that the source of the “enhancement” of the two-phonon ESWR compared to the value given by the harmonic limit is the violation of the condition $[\hat{D}, [\mathcal{V}, \hat{D}]] = 0$ for the interaction part \mathcal{V} of the model Hamiltonian and the operator \hat{D} generating the electromagnetic transition. As a result, the EWSR for the two-phonon excitation exceeds its value in the harmonic limit by a factor of ~ 1.8 at $N \approx 136$ and $\chi = 0.8$. It is also shown that the energy shift of the two-phonon energy compared to its value in the harmonic limit decreases with increasing the particle number N following a power law, which is more complicated than the simple approximation $\sim N^{-x}$. The RPA and RRPA underestimate the exact EWSR of the two-phonon excitation by about 30% at a given interaction in the region where the RPA is valid.

DOI: 10.1103/PhysRevC.65.034325

PACS number(s): 24.30.Cz, 21.60.Jz, 23.20.-g

I. INTRODUCTION

The double giant dipole resonance (DGDR) has been observed recently in the relativistic heavy-ion reactions via Coulomb excitation [1–3] and pion-induced charge-exchange reactions. The results of these experiments are kind of controversial with respect to the conventional understanding of multiphonon resonances within the independent-phonon picture (IPP) (also called the harmonic limit). According to the latter, a DGDR is assumed to be a two-dipole-phonon resonance, which is a giant dipole resonance (GDR) built on top of another GDR. As such, the DGDR parameters can be calculated by folding two independent GDRs [4]. Hence, the DGDR energy E_{DGDR} is expected to be $2E_{\text{GDR}}$ (E_{GDR} is the GDR energy), and the DGDR full width at the half-maximum Γ_{DGDR} is equal to $2\Gamma_{\text{GDR}}$ (Γ_{GDR} is the GDR FWHM), if folding Lorentzian photoabsorption cross sections is used, or to $\sqrt{2}\Gamma_{\text{GDR}}$, if Gaussians are folded. In reality, because of the anharmonicities, the energy and width of DGDR will differ slightly from these values. This feature has been observed in experiments [2,3], where it has been found that the energy shift $\Delta E \equiv 2E_{\text{GDR}} - E_{\text{DGDR}}$ is few hundred keV for ^{136}Xe , while a relation $\sqrt{2}\Gamma_{\text{GDR}} \leq \Gamma_{\text{DGDR}} \leq 2\Gamma_{\text{GDR}}$ holds. However, the controversy is seen in the value of the experimentally extracted cross section of electromagnetic (EM) (or Coulomb) excitation for the DGDR, which turns out to be much larger than that given by the folding model. The “enhancement” is found to be around 178–200% in the reactions with ^{136}Xe projectiles at 700-MeV/nucleon kinetic energy [3], and around 133% using ^{208}Pb projectiles at 640-MeV/nucleon kinetic energy, bombarding ^{208}Pb target [2]. Several microscopic approaches have been recently developed to study the multiphonon giant

resonances [5], however none of them can describe the “enhancement” of the DGDR cross section without artificially increasing the GDR integrated strength to a value much higher than the experimental one. Recently, the phonon damping model (PDM), proposed in [6], has been applied to calculate the multiple-phonon resonances [7–9]. The PDM can describe the EM cross sections of DGDR simultaneously for both ^{136}Xe and ^{208}Pb cases along with the DGDR width and energy [9]. Since the PDM uses two phenomenological parameters to reproduce the GDR, a question still remains on the reason why the other microscopic models strongly underestimate the EM cross section of the DGDR. The aim of the present work is to shed light on this issue. For the clarity of the answer it is desirable to use a simple but exactly solvable model, with which the results of well-established microscopic approaches, such as the random-phase approximation (RPA), can be compared with. A candidate is the Lipkin-Meskov-Glick (LMG) [10] model, which has been widely used in literature to test the validity of various many-body approximation methods. The LMG model was used recently to study the anharmonicity in the energy of the single- and double-phonon states in Ref. [11], where, however, the “enhancement” in the energy-weight sum rule (EWSR) of the DGDR was not considered.

The paper is organized as follow. Section II discusses the EWSR of the double-phonon excitation and its application to the LMG model. Section III analyzes the results of numerical calculations. The last section summarizes the paper, where conclusions are drawn.

II. ENERGY-WEIGHT SUM RULE OF DOUBLE-PHONON EXCITATION WITHIN THE LMG MODEL

The quantity that is directly related to the integrated cross section of any resonance is its EWSR S_1 . If the resonance states are generated by Hermitian operator \hat{O} in a system described by a Hamiltonian H with a two-body interaction \mathcal{V} ,

*Electronic address: dang@rikaxp.riken.go.jp

the EWSR is defined by the identity [12,13]

$$S_1 \equiv \sum_{\nu} (E_{\nu} - E_0) |\langle \nu | \hat{O} | 0 \rangle|^2 = \frac{1}{2} \langle 0 | [\hat{O}, [H, \hat{O}]] | 0 \rangle, \quad (1)$$

where $\{|\nu\rangle\}$ is the complete set of exact eigenstates with energies E_{ν} of H . In the case of the GDR, \hat{O} is the dipole operator $\hat{O} = \hat{D}$, so if the potential \mathcal{V} in the Hamiltonian commuted with \hat{D} , the right-hand side (RHS) of Eq. (1) would be equal to $NZ/(2MA)$ independently of models and of the structure of the ground state $|0\rangle$ [14]. One then obtains from Eq. (1) the well-known Thomas-Reich-Kuhn (TRK) sum rule for the GDR, $S_1^{(1)} = NZ/(2MA)$. Proceeding in the same way for DGDR by putting $\hat{O} = \hat{D}^2$, and evaluating the RHS of Eq. (1), it is easy to show [15] that

$$S_1^{(2)} = 4 \frac{NZ}{2MA} \langle 0 | \hat{D}^2 | 0 \rangle \equiv 4S_1^{(1)} S_0^{(1)}, \quad (2)$$

provided the following condition holds:

$$\mathcal{D} \equiv [\hat{D}, [\mathcal{V}, \hat{D}]] = 0. \quad (3)$$

Since the EWSR $S_1^{(1)}$ and non-EWSR $S_0^{(1)}$ of the GDR are known, the unknown EWSR $S_1^{(2)}$ of the DGDR on the LHS of Eq. (2) cannot exceed the value in its RHS. Hence, there is no way to get any enhancement of the DGDR strength compared to the results of the IPP obtained by folding two GDRs, as the latter satisfies the RHS of Eq. (2) [15]. However, in reality, as has been pointed out by us previously [8,16], the condition (3) does not hold within a general many-body Hamiltonian. Therefore, instead of Eq. (2), the EWSR $S_1^{(2)}$ for the double-phonon state is calculated as

$$\tilde{S}_1^{(2)} = S_1^{(2)} + \Delta S_1^{(2)}, \quad (4)$$

where the ‘‘enhancement’’ $\Delta S_1^{(2)}$ [compared with the case when Eq. (3) holds] is

$$\Delta S_1^{(2)} = \frac{1}{2} (\langle 0 | \hat{D}^2 \mathcal{D} | 0 \rangle + 2 \langle 0 | \hat{D} \mathcal{D} \hat{D} | 0 \rangle + \langle 0 | \mathcal{D} \hat{D}^2 | 0 \rangle), \quad (5)$$

which is obtained as a result of the exact calculation of the RHS of Eq. (1) when $\mathcal{D} \equiv [\hat{D}, [\mathcal{V}, \hat{D}]] \neq 0$. It is important to point out that, because of the complete set of the intermediate single-phonon states, the ‘‘enhancement’’ (5) does not depend on the reaction mechanism, which forms the double-phonon excitation. Hereafter, we will call the EWSR $S_1^{(2)}$ (2) the harmonic limit of $\tilde{S}_1^{(2)}$ (4) because the EWSR of two-phonon excitation within the IPP obtained by folding two GDRs satisfies this sum rule value $S_1^{(2)}$. A good quantity showing the deviation of the EWSR from the harmonic limit is the ratio

$$R = \frac{\tilde{S}_1^{(2)}}{S_1^{(2)}} \equiv 1 + \frac{\Delta S_1^{(2)}}{S_1^{(2)}}, \quad (6)$$

which reaches the value 1 in the harmonic limit, at which $\Delta S_1^{(2)}$ vanishes.

The Hamiltonian of the LMG model [10] is

$$H = T + \mathcal{V}, \quad T = \epsilon K_0, \quad \mathcal{V} = -\frac{1}{2} V (K_+^2 + K_-^2), \quad (7)$$

where the operators

$$K_0 = \frac{1}{2} \sum_{m=1}^N (a_{+m}^{\dagger} a_{+m} - a_{-m}^{\dagger} a_{-m}),$$

$$K_+ = \sum_{m=1}^N a_{+m}^{\dagger} a_{-m}, \quad K_- = (K_+)^{\dagger} \quad (8)$$

are the usual SU(2) generators, satisfying the commutation relations [17]

$$[K_+, K_-] = 2K_0, \quad [K_0, K_{\pm}] = \pm K_{\pm}. \quad (9)$$

The exact energy eigenvalues E_i and eigenvectors of the Hamiltonian (7) are found by diagonalizing the tridiagonal matrix, whose nonvanishing elements in the space of states $|J, M\rangle$ with $-J \leq M \leq J$ ($J = N/2$) are

$$\langle J, M | H | J, M \rangle = \epsilon M,$$

$$\langle J, M \pm 2 | H | J, M \rangle$$

$$= -\frac{1}{2} V \sqrt{(J \mp M)[J^2 - (M \pm 1)^2]} (J \pm M + 2). \quad (10)$$

The one-body operator \hat{D} , which can generate the transition between the particle (p) and hole (h) levels in this model, is

$$\hat{D} = F(K_+ + K_-), \quad (11)$$

where F is the matrix element of the electromagnetic transition, which corresponds to \hat{D} . The general form of F is $F = e_{\text{eff}}^{(L)} r^L [Y_{LM}(\theta, \phi) + (-1)^M Y_{L-M}]/(1 + \delta_{M0})$. In the case of the dipole operator ($L = 1$), $e_{\text{eff}}^{(1)} = eN/A$ for protons, and $-eZ/A$ for neutrons. Using the commutators (9), it is obvious that \hat{D} does not commute with the two-body interaction part \mathcal{V} of the Hamiltonian (7), because

$$[\mathcal{V}, \hat{D}] = -FV(K_0 K_+ + K_+ K_0 - K_0 K_- - K_- K_0), \quad (12)$$

which is never zero at a given nonzero interaction parameter V . The double commutator \mathcal{D} (3) is not zero either. Instead, it is equal to

$$\mathcal{D} \equiv [\hat{D}, [\mathcal{V}, \hat{D}]] = 2F^2 V (K_+^2 + K_-^2 - K_+ K_- - K_- K_+ + 4K_0^2). \quad (13)$$

The nonzero value of the commutator (12) also leads to the violation of the TRK sum rule. However, under a certain approximation, the expectation value of this commutator in the ground state can be considered to be equal to zero, conserving the TRK sum rule, while it is not the case for the double commutator (13) (see Sec. 3 of [8]).

It is worth noticing that a nonlocal interaction is used in the LMG model. In realistic nuclei, it is well known that, if the GDR strength is integrated up to the meson thresholds at ~ 140 MeV, the EWSR exceeds the TRK sum rule by up to 0.4–0.5 TRK sum rule units. This enhancement is usually attributed to the contribution of the meson-exchange or velocity-dependent forces [12,14]. These forces also violate condition (3). However, the photoabsorption cross sections of GDR are usually measured up to 30 MeV, where the TRK sum rule is well exhausted for nuclei with mass numbers $A \geq 100$, while the electromagnetic cross sections for DGDR have been obtained within the energy interval up to 40 MeV. In this region of excitation energy the contribution of the exchange or velocity-dependent forces is expected to be small. On the other hand, the problem about the ratio between the nonlocal and explicit velocity-dependent elements in nucleonic potentials has been known for several decades [18]. Recent calculations of the triton binding energy with a high-precision nonlocal NN potential, which is derived from relativistic meson field theory, significantly reduces the discrepancy between theory and experiment established from local potential [19]. Other insights into the reaction mechanisms underlying the nuclear forces also suggest a nonlocal character rather than a local one [20].

A. Exact EWSR

The harmonic limit $S_1^{(2)}$ and the ‘‘enhancement’’ $\Delta S_1^{(2)}$ at the RHS of Eq. (4) are calculated exactly using the RHS of Eq. (1), and can be expressed in terms of the exact eigenvectors $a_M^{(\nu)}$ as

$$\begin{aligned} S_1^{(2)} &= \frac{1}{2} \langle 0 | [\hat{D}^2, [T, \hat{D}^2]] | 0 \rangle \\ &= \frac{1}{2} \sum_{MM'} a_M^{(0)} a_{M'}^{(0)} \langle J, M' | [\hat{D}^2, [T, \hat{D}^2]] | J, M \rangle, \end{aligned} \quad (14)$$

and

$$\begin{aligned} \Delta S_1^{(2)} &= \frac{1}{2} \sum_{MM'} a_M^{(0)} a_{M'}^{(0)} (\langle J, M' | \hat{D}^2 \mathcal{D} | J, M \rangle \\ &\quad + 2 \langle J, M' | \hat{D} \mathcal{D} \hat{D} | J, M \rangle + \langle J, M' | \mathcal{D} \hat{D}^2 | J, M \rangle). \end{aligned} \quad (15)$$

The matrix elements at the RHS of Eqs. (14) and (15) are calculated exactly making use of the commutators (9). The coefficients $a_M^{(0)}$ are the components of the exact eigenvector of the ground state ($\nu=0$), which is the state with the lowest energy E_0 from the set of the exact eigenstates $|\nu\rangle$ found by diagonalizing the Hamiltonian (7)

$$|\nu\rangle = \sum_M a_M^{(\nu)} |J, M\rangle. \quad (16)$$

Varying the interaction parameter V (or $\chi = NV/\epsilon$), one can see the behavior of the ratio R from Eq. (6) as a function

of $V(\chi)$. It is obvious that the harmonic limit is reached only at zero interaction ($V=0$), where $\Delta S_1^{(2)}$ from Eq. (15) vanishes.

B. EWSR within the renormalized RPA

The foundation of most microscopic approaches to nuclear collective excitations is the RPA. The coherent ph configurations across the Fermi surface are treated within the RPA as a collective phonon excitation. The conventional RPA equation is usually obtained within the quasiboson approximation, which violates the Pauli principles between the phonons, as the latter are considered as ideal bosons. In this way, only a part of ph correlations is included in the RPA ground states. This leads to the collapse of the RPA at a critical point, where it yields an imaginary solution. Several approaches were developed taking into account the ground-state correlations beyond the RPA to correct for this inconsistency [21–25]. One of them is the renormalized RPA (RRPA), proposed in [21], and improved recently in [25], within which a set of RPA-like equations is solved self-consistently with the equation for the single-particle occupation number.

Applying the RRPA method of [25] to the LMG model, we introduce the phonon operators Q^\dagger and Q as

$$Q^\dagger = XK_+ - YK_-, \quad Q = [Q^\dagger]^\dagger. \quad (17)$$

Using the exact commutators from Eq. (9), we can evaluate the average value of the commutator between Q and Q^\dagger in the correlated ground state $|\bar{0}\rangle$ as

$$\langle \bar{0} | [Q, Q^\dagger] | \bar{0} \rangle = -2(X^2 - Y^2) \langle \bar{0} | K_0 | \bar{0} \rangle = DN(X^2 - Y^2), \quad (18)$$

where the GSC factor D is defined as the difference between occupation numbers for holes ($n_- \neq 1$) and particles ($n_+ \neq 0$) in the correlated ground state,

$$D = n_- - n_+, \quad n_\pm = \langle \bar{0} | a_\pm^\dagger a_\pm | \bar{0} \rangle. \quad (19)$$

Therefore, if the phonon amplitudes X and Y satisfy the usual orthonormalization condition as that of the RPA, i.e.,

$$N(X^2 - Y^2) = 1, \quad (20)$$

the average value (18) of the commutator between phonons in the correlated ground state becomes

$$\langle \bar{0} | [Q, Q^\dagger] | \bar{0} \rangle = D. \quad (21)$$

This means that the renormalized phonon operators $\bar{Q}^\dagger = Q^\dagger/\sqrt{D}$ and $\bar{Q} = Q/\sqrt{D}$ satisfy the same commutation relation as that of the QBA, namely, $\langle \bar{0} | [\bar{Q}, \bar{Q}^\dagger] | \bar{0} \rangle = 1$. This is the essence of the RRPA method. The RPA is recovered when $D=1$ (i.e., $n_- = 1$ and $n_+ = 0$).

The energy of the one-phonon state found as the solution of the RRPA equation within the LMG model is given as [25]

$$\omega_{\text{RRPA}} = \pm \epsilon \sqrt{1 - D^2 \chi^2}, \quad \chi = NV/\epsilon, \quad D = \frac{1}{1 + 2Y^2}. \quad (22)$$

The phonon X and Y amplitudes are

$$X = \sqrt{\frac{\epsilon + \omega}{2N\omega}}, \quad Y = \sqrt{\frac{\epsilon - \omega}{2N\omega}}. \quad (23)$$

Expressing the operators \hat{D} (11) and \mathcal{D} (13) in terms of phonon operators (17) using the inverse transformation

$$K_+ = N(XQ^\dagger + YQ), \quad K_- = N(YQ^\dagger + XQ), \quad (24)$$

we can calculate the EWSR for the two-phonon state, discussed in the preceding section, within the RRPA by replacing the exact ground state $|0\rangle$ with the RRPA one, $|\bar{0}\rangle$, for which $Q|\bar{0}\rangle = 0$. After some algebra, we obtain for the ‘‘enhancement’’ $\Delta S_1^{(2)}$ the following expression:

$$\begin{aligned} \Delta S_1^{(2)} = & 4F^4 ND\chi\epsilon \sqrt{\frac{1+D\chi}{1-D\chi}} \left[1 + ND^2 - D \sqrt{\frac{1-D\chi}{1+D\chi}} \right. \\ & + \frac{2}{N(1-D^2\chi^2)} \left[(1+D\chi)^2 - D\chi\sqrt{1-D^2\chi^2} \right. \\ & \left. \left. \times (1+ND^2) \right] \right]. \quad (25) \end{aligned}$$

The EWSR $S_1^{(1)}$ and non-EWSR $S_0^{(1)}$ for the one-phonon excitation $|1\rangle = Q^\dagger|\bar{0}\rangle$ within the RRPA are

$$\begin{aligned} S_1^{(1)} = & \omega |\langle \bar{0} | Q \hat{D} | \bar{0} \rangle|^2 = F^2 N \epsilon D^2 (1 + D\chi), \\ S_0^{(1)} = & |\langle \bar{0} | Q \hat{D} | \bar{0} \rangle|^2 = F^2 ND^2 \sqrt{\frac{1+D\chi}{1-D\chi}}. \quad (26) \end{aligned}$$

Using Eqs. (25) and (26), we can easily calculate the ratio (6) within the RRPA to be compared with the exact result of Sec. II A in the following section.

III. ANALYSIS OF NUMERICAL RESULTS

The exact excitation energies $E^{(i)} \equiv E_i - E_0$ for $i = 1$ and 2 are plotted as a function of χ in Fig. 1 in comparison with the one-phonon energies $\omega^{(1)} = \omega$ and the double-phonon energy in the harmonic limit, $\omega^{(2)} \equiv 2\omega$, found within RPA (dotted lines) and RRPA (dashed lines) at various N . The RPA breaks down at $\chi = 1$, while the RRPA has solution at all χ . However, being the renormalization of the harmonic RPA, the RRPA still cannot include all the anharmonicities of the exact eigenstates, which include excitations higher than the first and the second ones as well as the mutual coupling between them. Therefore, the harmonic double-phonon energy, $\omega_{\text{RRPA}}^{(2)} = 2\omega_{\text{RRPA}}$ within RRPA, starts to deviate significantly from $E^{(2)}$ at $\chi > 1$, and especially at $\chi \geq \chi_{\text{crit}}$, where χ_{crit} denotes the point at which $E^{(2)}$ starts to increase with

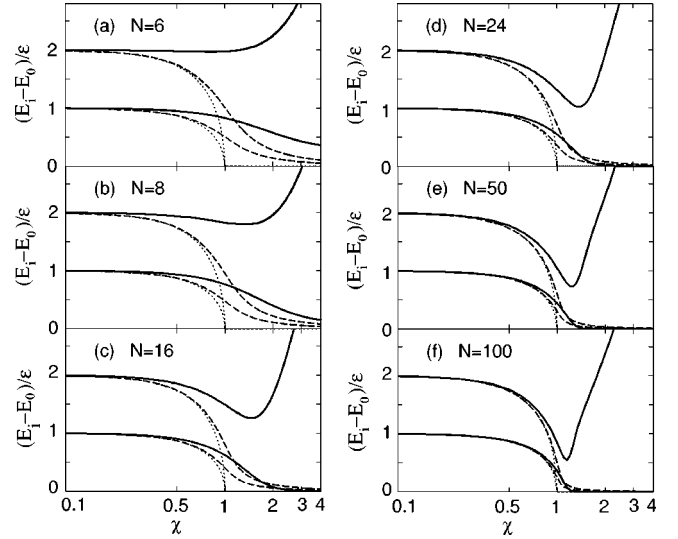


FIG. 1. Energies $E^{(i)} \equiv E_i - E_0$ (normalized to ϵ) of the first ($i = 1$) and second ($i = 2$) excited states relative to the ground state as a function of the interaction $\chi = NV/\epsilon$ at several values of N . The solid lines, which start from 1 and 2 at $\chi = 0$, denote the exact energies $E^{(1)}/\epsilon$ and $E^{(2)}/\epsilon$, respectively. The dotted lines denote the RPA one-phonon energy ω and double-phonon energy, $\omega^{(2)} \equiv 2\omega$. The corresponding RRPA energies are shown by the dashed lines.

increasing χ . It is around 1.1 for $N = 6$, 1.5 for $N = 8 - 24$, 1.25 for $N = 50$, and 1.2 for $N = 100$. At $\chi > \chi_{\text{crit}}$ the value $\omega_{\text{RRPA}}^{(2)}$, which becomes rather small and continues to decrease with increasing χ , fails short to match the exact eigenvalue $E^{(2)}$, which increases sharply. Defining the energy shift between the exact solution and that of the RPA (RRPA) as $\Delta E^{(i)} = E^{(i)} - \omega^{(i)}$, we see that this shift is significantly reduced at large N with $\Delta E^{(2)} > \Delta E^{(1)}$.

The energy shift $\Delta E^{(2)} = E^{(2)} - \omega^{(2)}$, which corresponds to the two-phonon excitation, is plotted as a function of χ at various values of N in Fig. 2. The double-phonon energy $\omega^{(2)} \equiv 2\omega$ is calculated within RPA (thin line) and RRPA

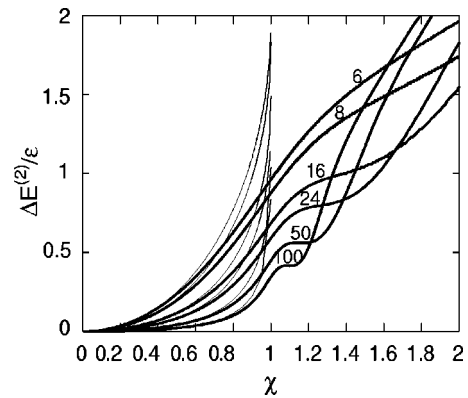


FIG. 2. Energy shift $\Delta E^{(2)} \equiv E^{(2)} - 2\omega$ (normalized to ϵ) as a function of the interaction parameter χ at various values of N . A thick line denotes the result obtained within RRPA, while the thin line adjacent to it stands for the corresponding result within RPA. The number on each thick line indicates the value of N at which the RRPA and RPA results are obtained.

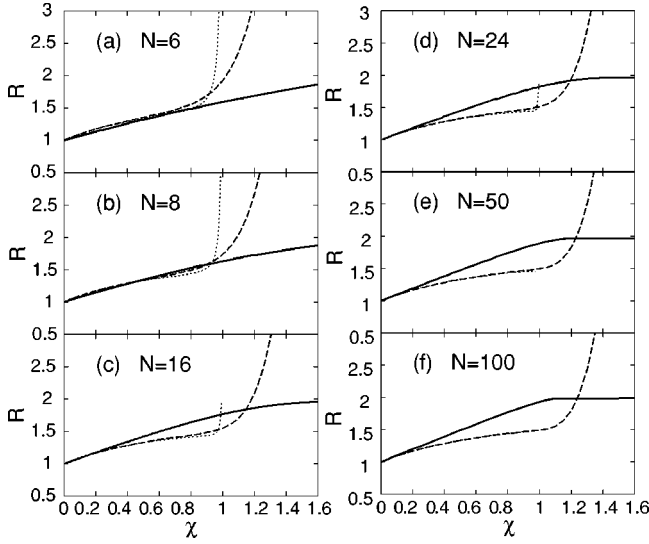


FIG. 3. Ratio R denoting the deviation of the EWSR for the two-phonon excitation from its value in the harmonic limit ($R = 1$) as a function of χ at various values of N . The solid line is the exact result, the dashed line shows the RRPA result, while the dotted line denotes the RPA result.

(thick line). It is seen in this figure that $\Delta E^{(2)}$ increases with increasing the interaction χ but decreases (at $\chi < 1.2$) as the particle number N increases. From this figure it is also clear that the shift of DGDR energy from the value given by the harmonic limit for ^{208}Pb should be smaller than for ^{136}Xe , because ^{208}Pb has a larger mass number and weaker interaction given the smaller width for GDR (about 4 MeV) in this nucleus. This feature has been experimentally confirmed [5]. However, it should be noted that the shift $\Delta E^{(2)}$ is always positive within the LMG model, while data from heavy-ion experiments show a negative $\Delta E^{(2)}$ for the DGDR peak in ^{136}Xe , and nearly a zero shift for the DGDR energy in ^{208}Pb . The two-phonon energy shift $\Delta E^{(2)}$ obtained in pion-exchange reactions is mostly positive within the error bars.

Already in Refs. [8,16] we have predicted that a small energy shift $\Delta E^{(2)}$ may correspond to a large deviation of the EWSR of the DGDR from the value given by the harmonic picture. This deviation is represented by the ratio R from Eq. (6) shown in Fig. 3 as a function of χ at various N . The harmonic limit corresponds to the value $R = 1$, which can be reached only at $\chi = 0$ as seen in the figure. At all $\chi \neq 0$, this ratio R is greater than 1, showing the “enhancement” of the two-phonon strength relative to its value given by the IPP. This “enhancement” increases with increasing the interaction parameter χ . For light systems ($N \leq 8$), the predictions by both of the RPA and RRPA are very close to the exact result in the region where the RPA is valid (i.e., at $\chi < 1$). At larger N the RPA and RRPA start to underestimate the exact result, and the discrepancy increases with increasing N . At $N = 100$, e.g., the “enhancement” given by the exact result is 1.77 times at $\chi \approx 0.8$, while the one obtained within the RPA, which nearly coincides with that of the RRPA, is only 1.45 times. Beyond the region of validity of RPA (at $\chi > 1$) the RRPA, which gives a sharp increase in the EWSR, fails to match the exact result.

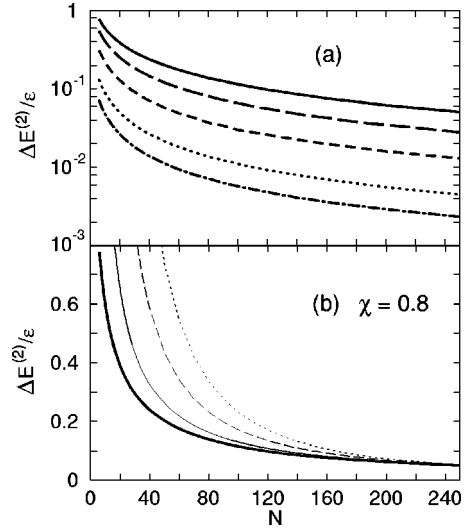


FIG. 4. Energy shift $E^{(2)} \equiv E^{(2)} - 2\omega_{\text{RPA}}$ (normalized to ϵ) as a function of particle number N at several $\chi < 1$ (a), and at $\chi = 0.8$ (b). In (a), the (thick) solid, long dashed, short dashed, dotted, and dash-dotted lines represent the results obtained at $\chi = 0.8, 0.7, 0.55, 0.4$, and 0.3 , respectively. In (b), the thick solid line is the same as that of (a) but plotted in the linear scale. The thin solid, dashed, and dotted lines are obtained using the dependence N^{-x} with $x = 1, 4/3$, and $5/3$, respectively (see the text).

There has been a number of discussions in literature about the dependence of the energy shift $\Delta E^{(2)}$ and the “enhancement” of the cross section for DGDR as a function of the mass number A (particle number N in the present LMG model). For $\Delta E^{(2)}$, this dependence has been assumed to be of the order of $\Delta E^{(2)} \sim N^{-x}$. Several values for x , such as $x = 1, 4/3$, or $5/3$, have been proposed within different approaches, and the final answer has not yet been reached [11,26]. To shed light on this issue we show in Fig. 4 the energy shift $\Delta E^{(2)} = E^{(2)} - 2\omega_{\text{RPA}}$ plotted as a function of N as several values of the interaction parameter $\chi < 1$. At a given interaction χ the decrease of $\Delta E^{(2)}$ with increasing N is rather weak for heavy systems ($N \geq 80$). We found that the dependence of $\Delta E^{(2)}$ on N can be precisely fitted with a polynomial curve using least square, $y = \beta_0 + \beta_1 N^{-1/3} + \beta_2 N^{-2/3} + \beta_3 N^{-1} + \beta_4 N^{-4/3} + \beta_5 N^{-5/3}$. The values of the coefficients β_i vary with varying χ , e.g., at $\chi = 0.8$, we found $\beta_0 = 1.88 \times 10^{-2}$, $\beta_1 = -0.43$, $\beta_2 = 3.01$, $\beta_3 = 9.57$, $\beta_4 = -25.53$, and $\beta_5 = 16.40$. Neither $x = 1, -4/3$, nor $-5/3$ alone can fit the result at all N . This is shown in Fig. 4(b) where the energy shift $\Delta E^{(2)}$ obtained at $\chi = 0.8$ is shown as a thick solid line together with the dependence $\sim N^{-x}$ obtained with $x = 1$ (thin solid line), $4/3$ (dashed line), and $5/2$ (dotted line). The curves given by $\sim N^{-x}$ are fitted to the value of $\Delta E^{(2)}$ at $N = 250$. It is seen from Fig. 4(b) that the dependence N^{-x} with $x = 1, 4/3$, and $5/3$ becomes a good approximation only at large $N \geq 180-200$. This analysis, however, is made at a given interaction parameter χ . As has been mentioned previously, the interaction decreases toward heavier systems. Therefore, it is expected that the dependence of $\Delta E^{(2)}$ on N will be steeper.

In order to obtain a calibration of the dependence of $\Delta E^{(2)}$ on both N and χ , we study the exact result for the ratio

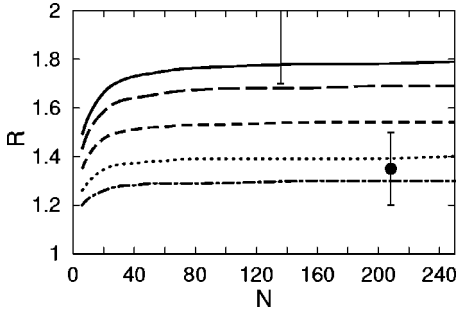


FIG. 5. The exact result for the ratio R as a function of N at $\chi = 0.8$ (solid line), 0.7 (long dashed line), 0.55 (short dashed line), 0.4 (dotted line), and 0.3 (dash-dotted line). The full circle with error bar at $N=208$ is the experimental value of R obtained for DGDR in ^{208}Pb . The experimental value of R for DGDR in ^{136}Xe is shown by the vertical line at $N=136$, whose center at $R=2.4$ is beyond the scale.

R as a function of N , which is plotted in Fig. 5 for several values of χ . This figure shows a rather weak dependence of the “enhancement” R of the two-phonon EWSR on the particle number N at each value of the interaction parameter χ , except for the region of light systems ($N \leq 20$). Also shown in this figure are the experimental values of R obtained for DGDR in ^{136}Xe and ^{208}Pb [1–3,5,26]. From here we conclude that the main reason for the large “enhancement” of the DGDR cross section for ^{136}Xe (more than 1.7 times compared to the harmonic limit) is that the anharmonicities in this nucleus must be large, which are caused, in part, by a large interaction $\chi \geq 0.8$. For the DGDR in ^{208}Pb the anharmonicities are much weaker, which correspond to $\chi \approx 0.3$ – 0.4 .

Going back to Fig. 4(a), we now see that, with increasing the particle number from $N \sim 130$ to $N \sim 200$, the real dependence of $\Delta E^{(2)}/\epsilon$ should move from the top curve (solid) downward to the bottom one (dash-dotted). However, even in this case, none of the values of $x=1$, $4/3$, nor $5/3$ can reproduce this slope. For example, the dependence $(\Delta E^{(2)}/\epsilon)_{\text{fit}} = 62N^{-4/3}$ ($x=4/3$) can fit the value of $\sim 8.8 \times 10^{-2}$ at $N=136$ obtained at $\chi=0.8$. However, it overestimates the value of $\Delta E^{(2)}/\epsilon$ at $N=200$ – 210 obtained at $\chi=0.3$ by a factor of 14. With the dependence $\sim N^{-1}$ ($x=1$) only one of the curves $\Delta E^{(2)}$ obtained at $\chi=0.8$ and $\chi=0.3$ can be roughly fitted using a coefficient of $(12-13)$ or $(12-13) \times 10^{-1}$, respectively [see, e.g., the thin solid line from Fig. 4(b)].

This analysis suggests that the interaction part \mathcal{V} of the Hamiltonian, for which the condition (3) does not hold, is the source of the large “enhancement” of the observed DGDR cross section for ^{136}Xe (about 1.7–2.0 times compared to the harmonic limit), and ^{208}Pb (about 1.3 times), as well as of the energy shift $\Delta E^{(2)}$. Based on this we can understand why some microscopic models underestimate the experimental DGDR cross sections. First of all, we have seen that, even if the interaction part \mathcal{V} were properly included, the use of the RPA or RRPA phonon operators would still underestimate the DGDR strength in the region of validity of RPA ($\chi < 1$) (see Fig. 5). Therefore, it is necessary to go beyond the

RPA and RRPA, taking into account two-, three-, or more-phonon configurations, in order to include anharmonicities properly. However, if the approximation is such that $\Delta S_1^{(2)}$ vanishes, i.e., the condition (3) still holds, the inclusion of more complex configurations can change only the spreading (the width) and may slightly shift the energy centroid of the resonance distribution, but not the EWSR significantly because of Eq. (2). For instance, it is easy to see that the condition (3) does not hold for the interaction part \mathcal{V} in the original Hamiltonian of the quasiparticle-phonon model (QPM) [27] because of the Fermion structure of the scattering quasiparticle pairs $[\alpha_j^\dagger \otimes \alpha_{j'}]_{\lambda\mu}$ and the phonon operators. However, in the calculations of the coupling to two- and three-phonon configurations within the QPM, an approximation has been made, which is equivalent to expressing the scattering quasiparticle pairs in terms of the sum of the products of two phonon operators $\sim Q_{\lambda\mu i}^\dagger Q_{\lambda\mu i}$. While this approximation is sufficient for studying the spreading of the GDR preserving its EWSR, it makes the average of the double commutator at the LHS of Eq. (3) over the ground state vanish, because the number of phonon operators in the average is always odd, just losing the strength $\Delta S_1^{(2)}$ of the DGDR. Therefore, the calculations within the QPM failed to describe the experimental cross section of the DGDR despite the inclusion of a large basis with one-, two-, and even three-phonon components in the wave function (see the review in Sec. 2.3 of [5]). At the same time, we can see why the PDM [6] can describe well the cross section of the DGDR for both ^{136}Xe and ^{208}Pb in good agreement with the experimental data [9]. The PDM uses a phenomenological dipole phonon (not RPA phonon), whose unperturbed energy and coupling parameter to ph configurations are adjusted to describe well the GDR. In the process of calculating the DGDR using the same set of parameters for GDR within the PDM, the average value of the LHS of Eq. (3) remains finite [8].

IV. CONCLUSIONS

This work studies the EWSR and energy of the two-phonon excitation, including the DGDR as a special case, within the LMG model as a function of the interaction at various particle numbers. The Hamiltonian of this exactly solvable model has such an interaction part \mathcal{V} that neither $[\mathcal{V}, \hat{D}]$ nor $[\hat{D}, [\mathcal{V}, \hat{D}]]$ is zero for the operator \hat{D} , which generates the electromagnetic transition. The exact solutions for the first and second excited states above the ground state, obtained within the LGM model, are used to estimate the deviation of the two-phonon EWSR from the prediction by the IPP (the harmonic limit), and to compare with the predictions given within the RPA and RRPA.

The analysis of the results obtained allows us to draw the following conclusions.

(i) The source of the “enhancement” $\Delta S_1^{(2)}$ of the two-phonon EWSR compared to the prediction $S_1^{(2)}$ given by the harmonic limit is the violation of the condition (3). At a given particle number N , this “enhancement” increases with increasing the interaction parameter χ . As a result the EWSR $S_1^{(2)}$ for the two-phonon excitation may exceed its value in the harmonic limit by a factor $R \approx 1.8$ at $N \approx 136$ and

$\chi=0.8$ (region of ^{136}Xe), or $R\approx 1.3$ at $N\approx 208$ and $\chi=0.3$ (region of ^{208}Pb). Although these values agree with the experimental findings of the “enhancement” of the DGDR cross section compared to the values given within the harmonic limit for ^{136}Xe and ^{208}Pb , a rigorous comparison between the results obtained within the LMG and the experimental data is not possible as a number of effects such as angular momentum, isospin, and parity, etc., are left out in such a simple model. On the other hand, it is clear that this model can be used as a testing ground to check various theoretical approaches to the DGDR.

(ii) The energy shift $\Delta E_1^{(2)}$ of the two-phonon energy compared to its value in the harmonic limit is always positive within the LMG model. It decreases with increasing the particle number N following a power law, which is more complicated than the simple approximation $\sim N^{-x}$ with $x=1, 4/3, \text{ or } 5/3$.

(iii) The EWSR for the two-phonon state, which is con-

structed of two RPA and RRPA one-phonon states within the LMG model underestimate the exact EWSR of the two-phonon excitation by about 30% at a given interaction parameter χ within the region of validity of the RPA ($\chi < 1$).

(iv) In order to describe correctly the cross section for two-phonon excitations within a microscopic model, the approximation should be made in such a way as to include the anharmonicities beyond the RPA preserving the nonzero value of the double commutator $[\hat{D}, [\mathcal{V}, \hat{D}]]$.

ACKNOWLEDGMENTS

Sincere thanks are due to V. Zelevinsky (MSU) for carefully reading the manuscript and valuable comments. The numerical calculations were carried out using the FORTRAN IMSL Library by Visual Numerics on the Alpha server 800 5/500 at the RIKEN Division of Computer and Information.

-
- [1] R. Schmidt *et al.*, Phys. Rev. Lett. **70**, 1767 (1993).
 [2] K. Boretzky *et al.*, Phys. Lett. B **384**, 30 (1996).
 [3] K. Boretzky *et al.* (unpublished); Phys. Rev. C **60**, 051601 (1999).
 [4] W.J. Llope and P. Braun-Munzinger, Phys. Rev. C **41**, 2644 (1990).
 [5] T. Aumann, P.F. Bortignon, and H. Emling, Annu. Rev. Nucl. Part. Sci. **48**, 351 (1998).
 [6] N.D. Dang and A. Arima, Phys. Rev. Lett. **80**, 4145 (1998); Nucl. Phys. **A636**, 443 (1998).
 [7] N.D. Dang, K. Tanabe, and A. Arima, Phys. Rev. C **59**, 3128 (1999).
 [8] N.D. Dang, K. Tanabe, and A. Arima, Nucl. Phys. **A675**, 531 (2000).
 [9] N.D. Dang, V.K. Au, and A. Arima, Phys. Rev. Lett. **85**, 1827 (2000).
 [10] H.J. Lipkin, N. Meshkov, and A.J. Glick, Nucl. Phys. **62**, 188 (1965).
 [11] G.F. Bertsch, P.F. Bortignon, and K. Hagino, Nucl. Phys. **A657**, 59 (1999).
 [12] P. Ring and P. Schuck, *The Nuclear Many-Body Problem* (Springer, Berlin, 1980).
 [13] D.J. Thouless, *The Quantum Mechanics of Many-Body Systems* (Academic Press, New York, 1961).
 [14] A. deShalit and H. Feshbach, *Theoretical Physics, Nuclear Structure*, Vol. I (Wiley, New York, 1990).
 [15] H. Kurasawa and T. Suzuki, Nucl. Phys. **A597**, 374 (1996).
 [16] N.D. Dang, A. Arima, V.G. Soloviev, and S. Yamaji, Phys. Rev. C **56**, 1350 (1997).
 [17] A. Klein and E.R. Marshalek, Rev. Mod. Phys. **63**, 375 (1991).
 [18] A. Bohr and B.R. Mottelson, *Nuclear Structure* (Benjamin, New York, 1969), Vol. 1, p. 244.
 [19] R. Machleidt, F. Sammarruca, and Y. Song, Phys. Rev. C **53**, R1483 (1996).
 [20] P.J. Siemens and A.P. Vischer, Ann. Phys. (N.Y.) **238**, 129 (1995); **238**, 167 (1995).
 [21] K. Hara, Prog. Theor. Phys. **32**, 88 (1964); K. Ikeda, T. Udagawa, and H. Yamamura, *ibid.* **33**, 22 (1965).
 [22] D.J. Rowe, Phys. Rev. **175**, 1293 (1968); Rev. Mod. Phys. **40**, 153 (1968); Nucl. Phys. **A107**, 99 (1968).
 [23] A. Klein, R.M. Dreizler, and R.E. Johnson, Phys. Rev. **171**, 1216 (1968).
 [24] P. Schuck and S. Ethofer, Nucl. Phys. **A212**, 269 (1973); J. Dukelsky and P. Schuck, *ibid.* **A512**, 446 (1990).
 [25] F. Catara, N.D. Dang, and M. Sambataro, Nucl. Phys. **A579**, 1 (1994).
 [26] G.F. Bertsch and H. Feldmeier, Phys. Rev. C **56**, 839 (1997); I. Hamamoto, *ibid.* **60**, 054320 (1999); H. Emling, *Proceedings of the International Symposium on Quasiparticle and Phonon Excitations in Nuclei, 1999*, edited by N. Dinh Dang and A. Arima (World Scientific, Singapore, 2000), p. 54.
 [27] V.G. Soloviev, *Theory of Atomic Nuclei—Quasiparticles and Phonons* (IOP, Bristol, 1992).